Journal of Engineering Physics and Thermophysics, Vol. 71, No. 6, 1998

CALCULATION OF A SEPARATED LOW-VELOCITY AIR FLOW PAST A PROFILE WITH VORTEX CELLS

S. A. Isaev, Yu. S. Prigorodov, and
A. G. Sudakov

UDC 532.517.2

Solving two-dimensional Navier–Stokes equations on multiblock different-scale computational grids by a finite-volume method, we carry out numerical simulation of laminar low-velocity air flow past a profile with passive vortex cells.

One of the fundamental trends in present-day aerohydrodynamics is associated with control of flow past bodies using vortraps or cells, research on which has resulted in the creation of promising aircraft nontradtionally laid out aerodynamically (for example, the apparatus "Ékip"), which possess high aerodynamic quality due to a system of active (with air uptake) vortex cells. Solving the problem of optimization of the scheme considered made it possible to develop a mathematical model and a program package for predicting local and overall characteristics of flow past a profile of large thickness with several "passive" vortex cells located on the upper portion of the contour. The innovation of the formulation of this conjugate problem lies in the selection of multiblock computational regions with a substantial difference in the scales of flow inside of the cells and around the profile.

Numerical simulation of a two-dimensional uniform flow of an incompressible viscous liquid past a body is based on solving the system of Navier–Stokes equations for the laminar mode of flow. The problem is considered in a stationary formulation in a multiply connected region with account for flow separation. The differential equations are discretized by a finite-volume method on a curvilinear orthogonal grid of *O*-type generated on the basis of an algebraic procedure. The system of initial equations is written in a divergent form for the increments of the dependent variables: the Cartesian components of velocity and pressure.

The computational model suggested is based on the concept of splitting into physical processes, which is realized in the SIMPLEC procedure of pressure correction. The characteristic features of this iterative algorithm are determination of preliminary velocity components for "frozen" fields of pressure at the "predictor" step and subsequent correction of the pressure by solving a continuity equation with corrections of the velocity field. The computational process is constructed in such a way as to have several local iterative steps for one "predictor" step in the block of pressure correction.

The selection of a centered template with coupling of the dependent variables to the center of the computational cell is dictated by the desire to simplify the computational algorithm and to decrease the number of computational operations. Monotonization of the pressure field within the framework of this approach is carried out on the basis of the Rhee–Chou method. High stability of the computational procedure is ensured by applying one-sided countercurrent differences in the implicit portion of the equations for the increments of the dependent variables for discretization of the convective terms, damping of nonphysical oscillations by introduction of artificial diffusion, and use of pseudo-time stabilizing terms. The computational efficiency of the computational algorithm is related to the solution of systems of nonlinear algebraic equations by the method of incomplete matrix factorization in Stone's version (SIP). Acceptable accuracy of the procedure is ensured by discretization of the explicit portion of the equations following a scheme of second order of approximation and, in particular, by representing the convective terms of the equations according to Leonard's quadratic counter-current scheme (QUICK). The indicated methodology makes it possible to minimize the influence of the effects of "numerical" diffusion, which are especially substantial in calculation of separated flows. The details of the computational procedure are given in [1].

Academy of Civil Aviation, St. Petersburg, Russia. Translated from Inzhenerno-Fizicheskii Zhurnal, Vol. 71, No. 6, pp. 1116-1120, November-December, 1998. Original article submitted June 9, 1997.

 1062-0125/98/7106-1082$20.00

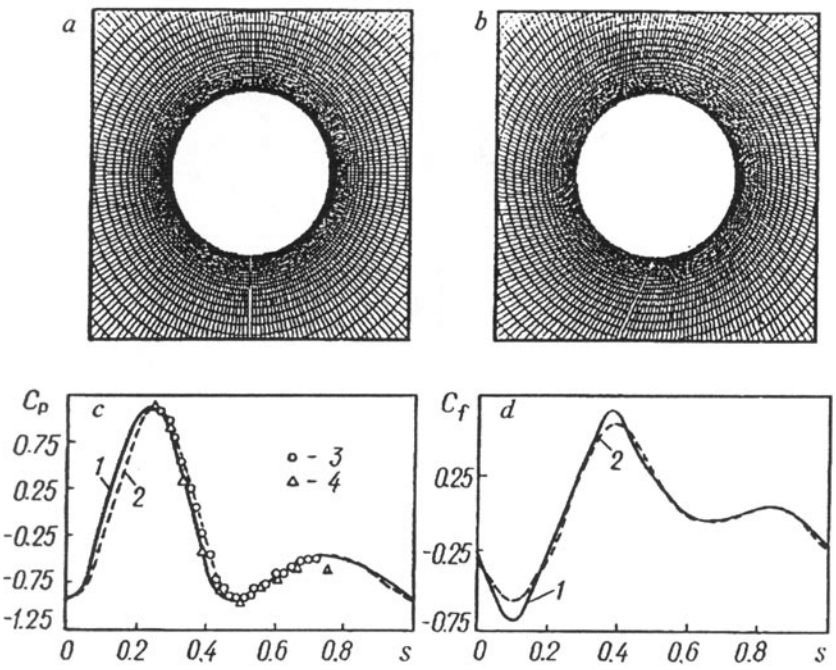

Fig. 1. Fragments of orthogonal (a) and oblique (b) computational grids of O-type near the cylinder and comparison of distributions of the coefficients of pressure C_p (c) and friction C_f (d) over the cylinder surface in a uniform flow of an incompressible viscous liquid at Re = 40: 1, 2) calculated results of the present work obtained on oblique and orthogonal grids, respectively; 3, 4) calculated results of Kawaguti and experimental data of Toma taken from the monograph of Batchelor [4].

TABLE 1. Comparison of Computed Results of Laminar Flow of an Incompressible Viscous Liquid Past a Cylinder at Re = 40

No. of the column	1	2	3	4
Type of grid	oblique	orthogonal	orthogonal	orthogonal
Number of cells	60 × 220	60 × 220	62 × 100	3000–4000
C_{xp}	0.408	0.398	–	–
C_{xd}	0.578	0.583	–	–
$C_{xp} + C_{xd}$	0.986	0.981	0.981	0.976
C_{xf}	0.541	0.517	0.5163	0.549
C_x	1.527	1.498	1.497	1.5025
C_{pf}	1.143	1.146	1.13	–
C_{pd}	−0.473	−0.473	−0.484	–
X_s	2.20	2.23	2.33	–

Note: Columns 1 and 2 contain results of the present work; 3 and 4 contain data taken from [2] and [3], respectively.

The testing of the algorithm developed was carried out on the problem of flow of a viscous incompressible liquid around a cylinder at Re = 40, and some of the results of its solution are presented in Fig. 1. Table 1 contains data for the overall characteristics of the flow around the cylinder, which were calculated using different algorithms and grids (polar and oblique, Fig. 1a, b). For purposes of comparison, the figure also contains results obtained by solving the Navier–Stokes equations written in transformed variables (vorticity–stream function). In [2] a finite-difference algorithm was constructed using Arakawa's scheme of 2nd and 4th order of approximation. A very fine computational grid was considered, which contained 62 × 100 nodal points. Earlier work [3] was carried out using

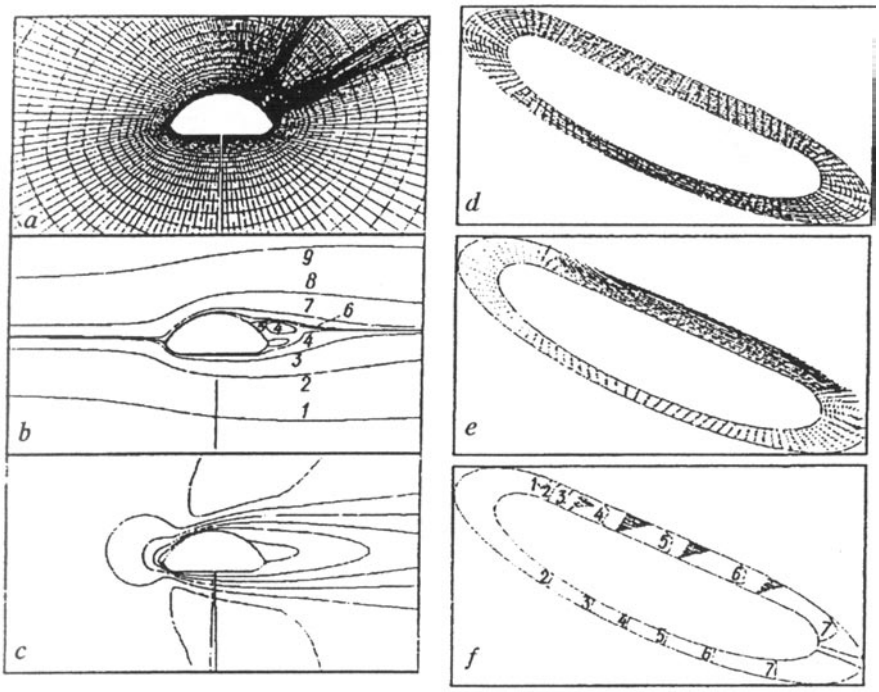

Fig. 2. Fragment of a grid constructed near a thick profile (a), picture of flow of an incompressible viscous liquid past a profile with a passive cell (b) at Re = 100 [1) $\psi = -0.5$; 2) −0.1; 3) −0.01; 4) −0.001; 5) 0; 6) 0.001; 7) 0.01; 8) 0.1; 9) 0.5]; picture of isotachs of the longitudinal (c) velocity component (the lines are drawn with a step of 0.2); computational grid in the passive vortex cell (d); picture of flow (e) and picture of isobars (f) [1) $p = -0.3$; 2) −0.29; 3) −0.28; 4) −0.27; 5) −0.26; 6) −0.25; 7) −0.24].

central finite differences, with the selected number of grid nodes being rather large (3000–4000). In addition to the results presented it should be noted that according to Apelt's data cited by Batchelor [4] $C_x = 1.513$, when Re = 40, whereas the experimental data of [5] show that the length of the circulation zone behind the cylinder X_s = 2.2.

From Table 1 and from the distributions of the pressure coefficients C_p in Fig. 1c it follows that all of the overall and local characteristics presented agree well among themselves and with the available experimental data. This means that in large measure the results of the numerical simulation of laminar flow around a cylinder are independent of the type of computational grid.

Some of the results obtained, which illustrate the efficiency of the created program complex, are presented in Figs. 2 and 3. The chord of the profile was selected as a characteristic dimension. Calculations of laminar flow past a thick profile (see Fig. 2a) in the presence and absence of a vortex cell of length 0.10 inserted into its afterbody (the angular position of the cell is shown in Fig. 2d) were performed for the ranges of the Reynolds number 50–800 and of the angle of attack 0–20°.

In the outer subregion the computational grid contained 61 × 221 cells nonuniformly distributed in a region of higher grid density in the vicinity of the body (Fig. 2a). The subregion of the vortex cell with the central body was divided into 10 × 100 cells (Fig. 2d) and was joined with the outer subregion via a common contact boundary. Transfer of information from one subregion to the other was carried out by means of linear reinterpolation of flows at the boundaries of the computational cells adjacent to the isolated contact boundary. First, convergence was attained in solving the problem in the outer subregion, and then, using the method of global iterations, the flow was calculated in both the outer field and the region of the vortex cell.

As follows from Fig. 2, the pattern of flow past the thick profile with the vortex cell at moderate Re numbers is characterized by the presence of a flow stagnation region in front of the body, rarefaction regions on the upper and lower sides of the profile, and formation of two large-scale vortices of different intensities in the region of flow

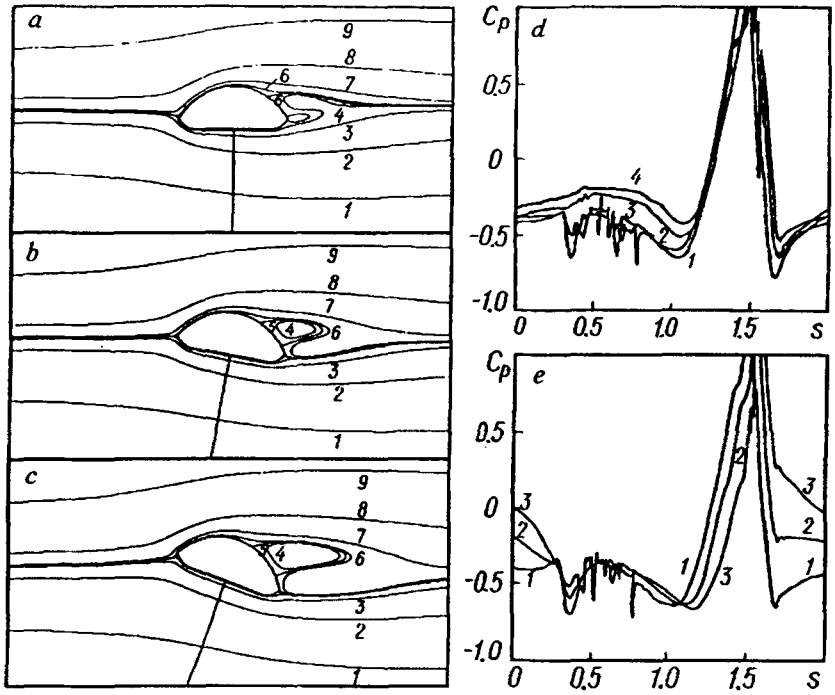

Fig. 3. Patterns of flow past a profile without vortex cells at Re = 100 for angles of attack of 0 (a), 10° (b), 20° (c) and graphs of the effect of the Reynolds number (d) and the angle of attack (e) on the distribution of the coefficient of pressure over the profile (counterclockwise), starting from the middle lower point of the profile: a, b, c: 1) $\psi = -0.5$, 2) -0.1, 3) -0.01, 4) -0.001, 5) 0, 6) 0.001, 7) 0.01, 8) 0.1, 9) 0.5; d: $\alpha = 0$: 1) Re = 50, 2) 100, 3) 400, 4) 800; e) Re = 100: 1) $\alpha = 0$; 2) 10°, 3) 20°.

separation in the near wake behind the profile. It should be noted that in the range of Reynolds numbers considered the pattern of flow around a profile with a cell almost does not differ from the pattern of flow around a profile without a cell. Probably, this is associated with the exceptionally weak flow in the vortex cell itself (Fig. 2e), which actually functions as a notch on the body surface. It is evident that for the intensity of the backward flow to be enhanced it is necessary to "activate" the cell by introducing a mechanism of injection and/or suction into action.

The change in the Reynolds number and the angle of attack as a whole leads to identical results associated with intensification of vortex flow in the near wake behind the profile (Fig. 3). Deformation of the vortex structure of the flow past the profile with a change in the angle of attack is responsible for the redistribution of local force loadings on the profile and an increase in the lift force.

Thus, a mathematical apparatus was developed and tested that is intended for solving the problem of controlling flow past bodies by means of vortex cells, and the necessity of using active means of action on the flow, in particular, on the basis of injection–suction was demonstrated.

The work was carried out with the support of the Russian Fund for Fundamental Research (grant 96-01-01290).

NOTATION

s, relative distance along the contour of the body measured counterlockwise; C_p, pressure coefficient; C_f, coefficient of friction; Re, Reynolds number; ψ, stream function; C_x, C_{xp}, C_{xd}, C_{xf}, coefficients of head, profile, bottom, and friction resistance; X_s, length of the separated region in the near wake behind the body; α, angle of attack. Subscripts: f, parameter at the forward stagnation point of the body; d, parameter in the bottom region behind the body.

REFERENCES

1. I. A. Belov, S. A. Isaev, and V. A. Korobkov, Problems and Methods of Calculation of Separated Flows of Incompressible Fluid [in Russian], Leningrad (1989).
2. I. A. Belov and N. A. Kudryavtsev, Heat Transfer and Resistance of a Bank of Tubes [in Russian], Leningrad (1986).
3. A. E. Hamielec and J. D. Raal, Phys. Fluids, 12, No. 1, 1013-1021 (1969).
4. J. Batchelor, Dynamics of Incompressible Viscous Fluid [Russian translation], Moscow (1973).
5. M. Coutanceau and R. Bouard, J. Fluid Mech., 79, Pt. 2, 257-272 (1977).